



**HAL**  
open science

# Halogen Bonds (N—I) at Work: Supramolecular Catemeric Architectures of 2,7-Dipyridylfluorene with ortho -, meta -, or para -Diiodotetrafluorobenzene Isomers

Ioana Georgeta Grosu, Lidia Pop, Maria Miclăuș, Niculina Daniela Hădade, Anamaria Terec, Attila Bende, Crina Socaci, Mihail Barboiu, Ion Grosu

## ► To cite this version:

Ioana Georgeta Grosu, Lidia Pop, Maria Miclăuș, Niculina Daniela Hădade, Anamaria Terec, et al.. Halogen Bonds (N—I) at Work: Supramolecular Catemeric Architectures of 2,7-Dipyridylfluorene with ortho -, meta -, or para -Diiodotetrafluorobenzene Isomers. *Crystal Growth & Design*, 2020, 20 (5), pp.3429-3441. 10.1021/acs.cgd.0c00205 . hal-03028976

**HAL Id: hal-03028976**

**<https://hal.science/hal-03028976>**

Submitted on 30 Nov 2020

**HAL** is a multi-disciplinary open access archive for the deposit and dissemination of scientific research documents, whether they are published or not. The documents may come from teaching and research institutions in France or abroad, or from public or private research centers.

L'archive ouverte pluridisciplinaire **HAL**, est destinée au dépôt et à la diffusion de documents scientifiques de niveau recherche, publiés ou non, émanant des établissements d'enseignement et de recherche français ou étrangers, des laboratoires publics ou privés.

# Halogen bonds (N---I) at work: supramolecular catemeric architectures of 2,7-dipyridylfluorene with *ortho*-, *meta*- or *para*-diiodotetrafluorobenzene isomers

*Ioana Georgeta Grosu,<sup>a#</sup> Lidia Pop,<sup>b#</sup> Maria Miclăuș,<sup>a</sup> Niculina D. Hădăde,<sup>b</sup> Anamaria Terec,<sup>b</sup>  
Attila Bende,<sup>a</sup> Crina Socaci,<sup>a</sup> Mihail Barboiu<sup>\*c</sup> and Ion Grosu<sup>\*b</sup>*

<sup>a</sup>National Institute for Research and Development of Isotopic and Molecular Technologies, 67-  
103 Donath str., RO-400293, Cluj-Napoca, Romania,

<sup>b</sup>Babes-Bolyai University, Faculty of Chemistry and Chemical Engineering, Department of  
Chemistry and SOOMCC, Cluj-Napoca, 11 Arany Janos str., 400028, Cluj-Napoca, Romania

<sup>c</sup>Institut Européen des Membranes, University of Montpellier, ENSCM-UM-CNRS UMR-5635,  
Pl. E. Bataillon, CC047, 34095, Montpellier, France.

#Joint first authors

KEYWORDS. Halogen bonds, N---I contacts, catemers, supramolecular architectures, single  
crystal X-ray structures.

ABSTRACT. Supramolecular assemblies of 2,7-dipyridylfluorene with diiodotetrafluorobenzene isomers were obtained by mechanochemical synthesis and their structures were determined by single crystal X-ray diffraction. The contribution of specific non-covalent interactions between different building blocks to the stability and solid-state packing behaviors of the supramolecular catemers was evaluated by theoretical methods, which confirm the geometries and interactional bonding observed in single crystal X-ray diffraction structures.

## Introduction

The non-covalent self-assembly of molecular building blocks toward complex supramolecular architectures is an exciting process. Their design gives access and investigation to interesting homo- and heteromolecular self-assembled “supramolecular architectures”. [1] The main non-covalent forces connecting such organic supramolecular assemblies are hydrogen-bonds, [2]  $\pi$  donor –  $\pi$  acceptor contacts, [3] hydrophobic interactions, [4] halogen bonds, [5] but in the large majority of the cases a plethora of contacts are synergistically contributing to the formation of supramolecular architectures. [6]

Of special interest, the investigation of halogen bonds [7] revealed several types of contacts involving halogen atoms and showed the important contribution of these interactions to stabilize supramolecular structures for which similar strength and directionality like of hydrogen bonds has been revealed. [5e] The X---N contacts (N belongs to a heteroaromatic ring; X is either I or Br) were investigated in finite structures (e.g. supramolecular cages or macrocycles, [8]) or in supramolecular polymers. [9] Difunctional halogen donors and difunctional halogen acceptors (e.g. compounds exhibiting two N heterocycles) prefer to form linear polymeric structures (catemers). [9] Many of these superstructures with unidimensional units were investigated in solid

state using single crystal X-ray diffraction. The results of solid-state investigations of X---N contacts were supported by theoretical calculations. [10] Among halogens, iodine gives the strongest contacts and the electron withdrawing groups as F atoms (e.g. in tetrafluorodiiodobenzene isomers versus the non-fluorinated diiodobenzenes) increase significantly the halogen donating ability of the derivatives.

In this context, we considered of interest to investigate the access, structure and properties of supramolecular architectures obtained from dipyridylarenes (I) as halogen acceptors and diiodobenzene or diiodo-tetrafluorobenzene derivatives (II) as halogen donors (Chart 1)

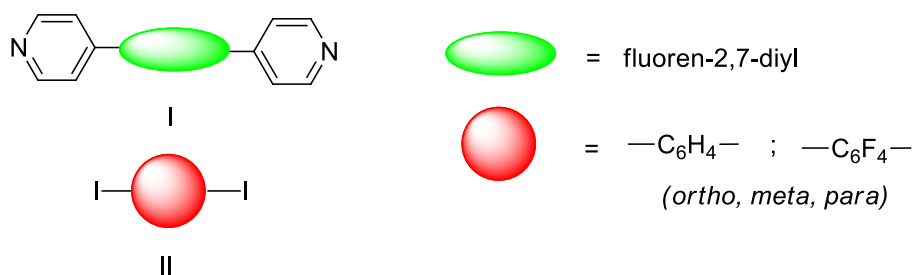


Chart 1. Selected building blocks for the access to halogen bonded supramolecular architectures

The ditopic halogen donors exhibit different binding geometries in correlation with the *ortho*-, *meta*- or *para*- positions of the iodine substituents, [11, 12] while the acceptor shows a quite linear disposition of the pyridine rings (Chart 2). Considering the geometries of the halogen donors and the ideal linear structure for the acceptor, the expected supramolecular assemblies formed by N---I contacts in the case of *p*-diiodobenzene ligands are linear polymers, while in the cases of *meta*- and *ortho*-diiodo derivatives the formation of hexagons or triangles in one side or 1D-zigzag polymer chains in the other side are taken into account (Chart 3). Literature data reveal the higher preference of *meta*- and *ortho*-diiodotetrafluorobenzene for zigzag polymers. [11-13]

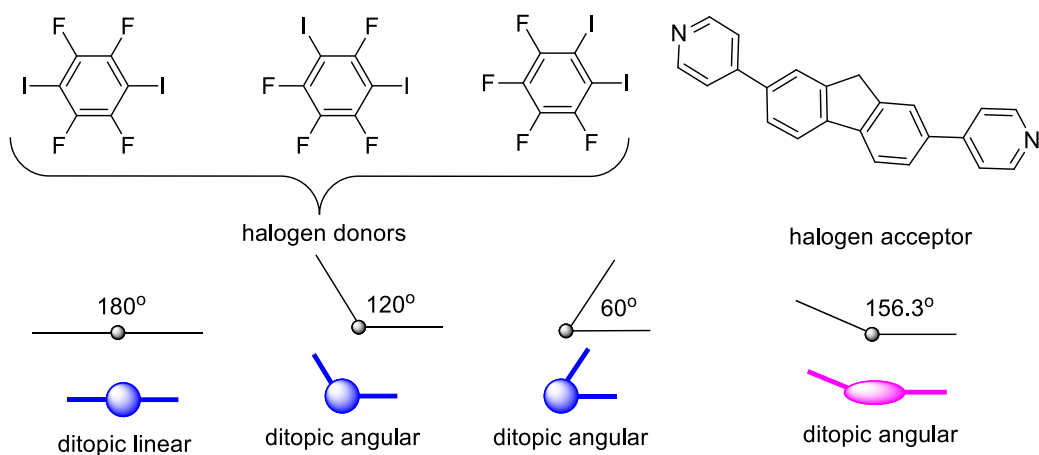


Chart 2. Binding geometries of the target halogen donors (linear or bent) and halogen acceptor [angular (determined from the single crystal X-ray diffraction structure of 2,7-dipyridyl-fluorene)]

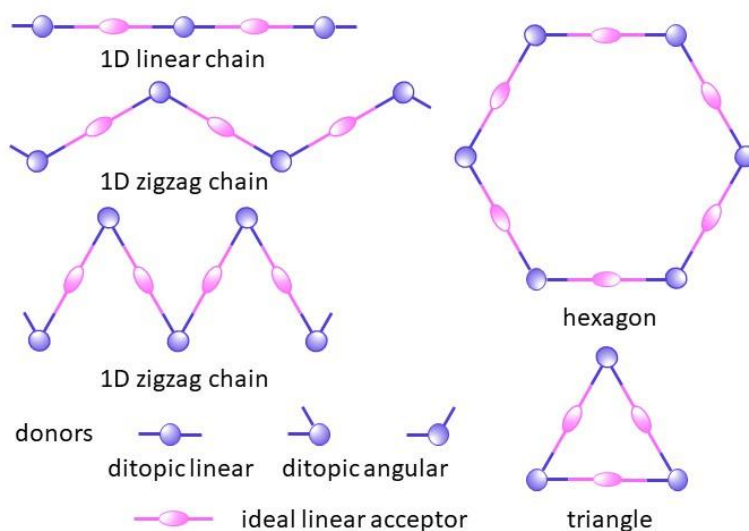
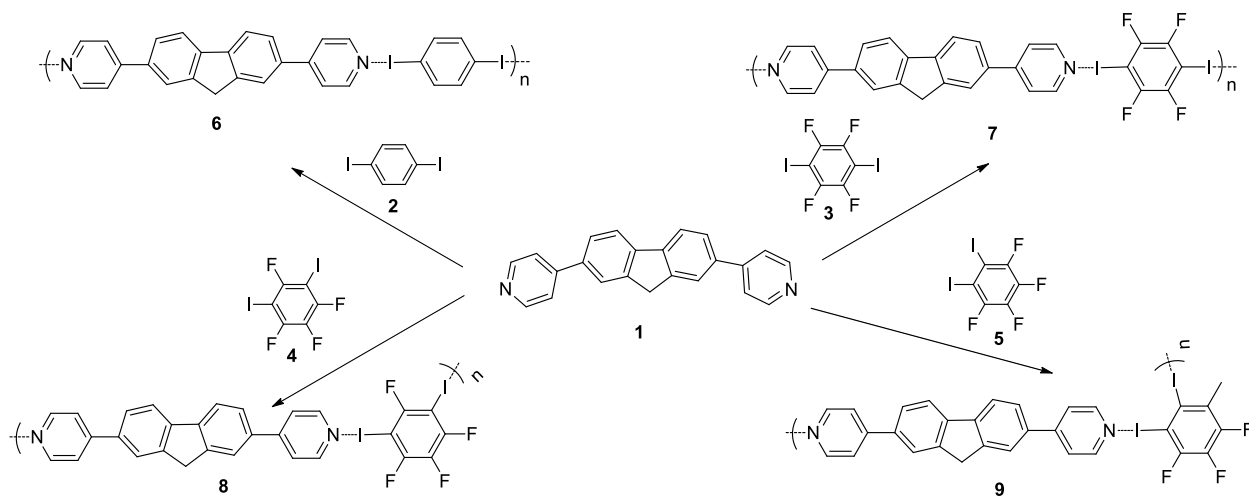


Chart 3. Expected supramolecular entities (1D linear, zigzag polymers or triangles and hexagons)

## Results and discussion

The supramolecular catemers **6-9** were obtained by the mechano-chemical solvent-drop grinding method (SCD) [14] starting from equimolar amounts (0.06 mmol) of 2,7-dipyridylfluorene-DPF (**1**) and *p*-diiodobenzene (**2**) and diiodotetrafluorobenzene isomers (**3-5**) (Scheme 1). Small

amounts (50  $\mu\text{L}$ ) of chloroform were added as solvent. The formation of the self-assembled products was monitored by powder X-ray diffractometry.



Scheme 1

The self-assembly of **1** with *meta*-diiodobenzene and *ortho*-diiodobenzene did not lead to the formation of specific halogen bonds and no supramolecular catemers were obtained.

Samples of **1** and **6-9** were solved in  $\text{CHCl}_3$  and crystals suitable for single crystal X-ray diffraction were obtained (in each case) by slow evaporation (*rt*) of the solvent.

In order to verify the compatibility of the bulk X-ray fingerprint with the single crystal structures, bulk powders of **6-9** were investigated by X-ray powder diffraction and they showed the same identity with the separated crystals (see SI).

The structure determination of supramolecular catemers in solid state is confirmed by single crystal X-ray diffractometry and FTIR spectroscopy and these results are in accord with theoretical calculations. Complex NMR investigations were also carried out in order to reveal the formation of halogen bonds in solution.

*Single crystal X ray diffraction structures and theoretical calculations for 1, 6-9*

The main goal of theoretical calculations was to estimate the contribution of different fragments of the lattice to the stabilization of crystal structures. For these purposes different fragments were extracted from the lattice and their calculated energy was compared with the energy of the system exhibiting the same molecules in isolated behavior.

Intermolecular interaction energies between different crystal fragments were determined at the local second-order Møller–Plesset (LMP2) perturbation theory level [15] together with the density fitting technique [16] implemented in the Molpro quantum chemistry program suite [17, 18]. The def2-TZVP [19] basis set for all atom cases together with the def2-ecp [20] effective core potential for the iodine atom were used for all calculations. In the framework of the LMP2 theory the effects of the basis set superposition error (BSSE) are substantially diminished [21], therefore their correction in the intermolecular interaction energy values were not taken into account. The theoretical calculations evaluate the diminishing of the energy in different crystal fragments (considered representative) compared to the energies of free molecules and they represent the global stabilization of the considered entities and it is not focused on the evaluation of the energetic stabilization brought individually by the different contacts observed in the lattice. The theoretical results are compared with experimental data and they are commented together with the discussion of X-ray diffraction structures. **The details of the theoretical calculations are shown in SI**

The single crystal X ray diffraction structures for **1** and **6-9** reveal the formation of different catemeric structures either by N---H-C(2') for **1** or N---I contacts for **6-9**. 2,7-DPF molecules are the halogen acceptors for **6-9** and they show slightly different structures, accordingly to their behavior in the lattice. In compounds **6**, **7** and **9** different types of 2,7-DPF molecules were observed and they were denoted with A and B for **6**, C and D for **7** and E, F and G for **9** and their characteristic data are shown in Table 1.

Table 1. Structural characteristics of 2,7-DPF molecules encountered in the single crystal X-ray diffraction structures of **1** and **6-9**

Compound	symbols	$\alpha$ ( $^{\circ}$ ) <sup>#</sup>	$\beta$ ( $^{\circ}$ ) <sup>#</sup>	$\gamma$ ( $^{\circ}$ ) <sup>#</sup>	Drawings
1	-	6	2.3	46	<b>Nu cred ca are rost</b>
6	A	6.7	30.4	39.1	<b>sa pun desenele aici</b>
	B	10.5	27.8	35.0	<b>ca o sa para toate la fel</b>
7	C	0	22.2	24.9	<b>Ce zici?????</b>  <b>Nu prea e clar ce e ecu</b>  <b>A B C direct din tabel</b>  <b>Dar formulele for fi</b>  <b>mai complicat de pus</b>
	D	0	20.9	23.2	
8	-	0	0.5	7.3	
9	E	0	16.2	24.2	
	F	0	14.9	24.5	
	G	0	24.1	27.5	

<sup>#</sup> $\alpha$  - dihedral angle between benzene rings;  $\beta$ ,  $\gamma$  - torsion angles of pyridine units

The results of the investigation of the structure of 2,7-dipyridylfluorene (2,7-DPF) itself are shown in Figure 1.

The analysis of the structure of **1** (Figure 1a) reveals a quite planar entity with a slight curvature of the fluorene units [the angle between the benzene rings is  $\alpha = 6^{\circ}$ ]. One of the



pyridine rings is almost coplanar with the connecting benzene ring (dihedral angle  $\beta = 2.3^\circ$ ), while the other one exhibits a dihedral angle  $\gamma = 45.9^\circ$ . In the lattice (Figure 1b) pairs of chains due to C-H...N connections are observed. The C(2')-H...N ( $d_{\text{H...N}} = 2.618 \text{ \AA}$ ) contacts rely the molecules of a chain, while the C(9)-H...N ( $d_{\text{H...N}} = 2.609 \text{ \AA}$ ) interactions are connecting the chains.

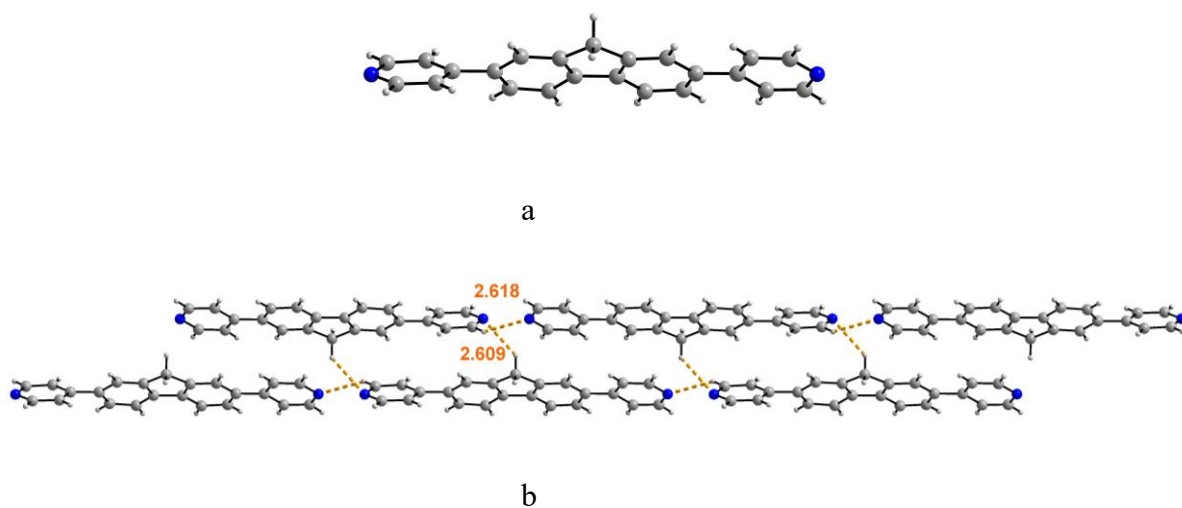
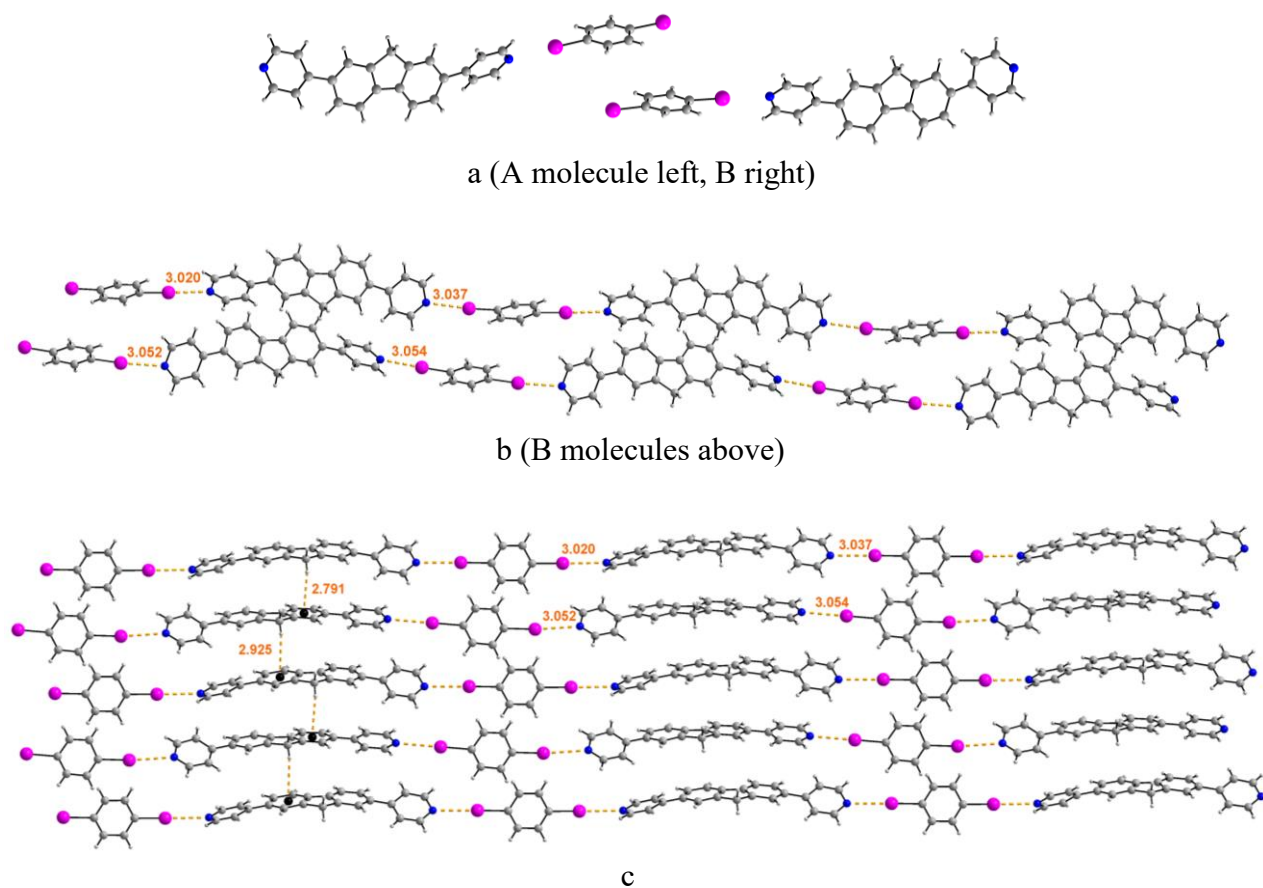


Figure 1. Single crystal X-ray diffraction results for **1**: molecular structure (a) and molecule disposal in the lattice (b)

The repetitive unit for **6** (Figure 2, a) reveals two different geometries for 2,7-dipyridylfluorene units connected to *p*-DIB counterparts. The curvatures of the fluorene units are somewhat higher than in **1** [the angles between the benzene rings are  $\alpha = 6.7$  (unit A) and  $10.5^\circ$  (unit B) respectively] and the pyridine rings exhibit different torsion angles with the connecting benzene entities [A:  $30.4$  ( $\beta$ ) and  $39.1$  ( $\gamma$ ); B:  $27.8$  ( $\beta$ ) and  $35.0^\circ$  ( $\gamma$ )].

In the lattice, the formation of endless catemeric chains by N...I halogen bonds is observed [ $d_{\text{N...I}} = 3.052$  and  $3.054 \text{ \AA}$  (for A molecules);  $d_{\text{N...I}} = 3.020$  and  $3.037 \text{ \AA}$  (for B molecules); Figure 2,b (B above)]. There are two types of N...I based chains (exhibiting either units A or units B of 2,7-DPF molecules) disposed alternatively in the lattice and they are connected one to each other by

C(sp<sup>3</sup>)-H---aromatic contacts [dC(9)-H---centroid Ph = 2.791 Å and 2.925 Å (Figure 2, c)] leading to infinite sheets (2D units). The sheets are interconnected to form 3D structures by additional C-H---aromatic contacts. The main C-H---aromatic interactions involve the centroid of benzene of neighboring 2,7-DPF and C(3)-H (3.116 Å) or C(2'')-H (3.066, 3.123 Å) and the centroids of 1,4-DIB molecules in contact with C(9)-H (2.999 Å), C(3')-H (3.096, 3.084 Å) and C(4)-H (2.991 Å) (Figure 2, d).



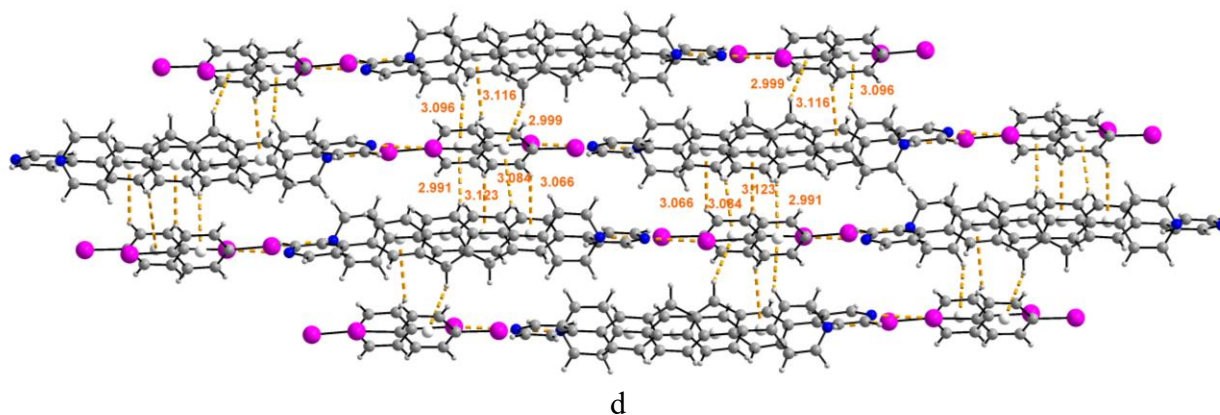


Figure 2. Single crystal X-ray structure of catemer **6**: repetitive unit (a); N---I catemers (b), 2D units (c) and 3D structure (d)

The theoretical calculations, in addition to the halogen-bond (N---I) interactions estimated to have  $-4.53$  kcal/mol intermolecular interaction energy per halogen-bond (Figure 2b), reveal significant contacts between the 2,7-DPF units belonging to different chains [exhibiting quite parallel fluorene rings and T-shaped pyridine ones (in a slightly slant conformation from the perfect perpendicular orientation), Figure 3a] with an estimated stabilization of  $-13.32$  kcal/mol.

The *p*-DIB molecules are bounded to these 2,7-DPF dimer units in two different T-shape configurations where the intermolecular interaction energy between 2,7-DPF and *p*-DIB are estimated to  $-5.18$  kcal/mol (Figure 3b) and  $-3.94$  kcal/mol (Figure 3c), respectively.

Dimer with A and B 2,7-DPF units (a)	T shape 2,7-DPF-DIB unit (b)	T shape 2,7-DIB-DPF unit (c)
$-13.32$ kcal/mol	$-5.18$ kcal/mol	$-3.94$ kcal/mol
Figure 3. Results of theoretical calculations for <b>6</b> ( $\Delta G^\circ$ )		

The repetitive unit of **7** (Figure 4, a) reveals two geometries of 2,7-DPF units connected to *p*-DITFB counterparts. The fluorene units are planar in this case and pyridine rings show slight torsion angles with the fluorene moieties [unit C: 22.2 ( $\beta$ ), 24.9 ( $\gamma$ ) and unit D: 20.9 ( $\beta$ ), 23.2° ( $\gamma$ )]. The 2,7-DPF and *p*-DITFB molecules form infinite chains (Figure 4b) of alternating C and D units *via* N---I halogen bonds (C:  $d_{\text{N---I}} = 2.893, 2.844$ ; D: 2.798; 2.827 Å).

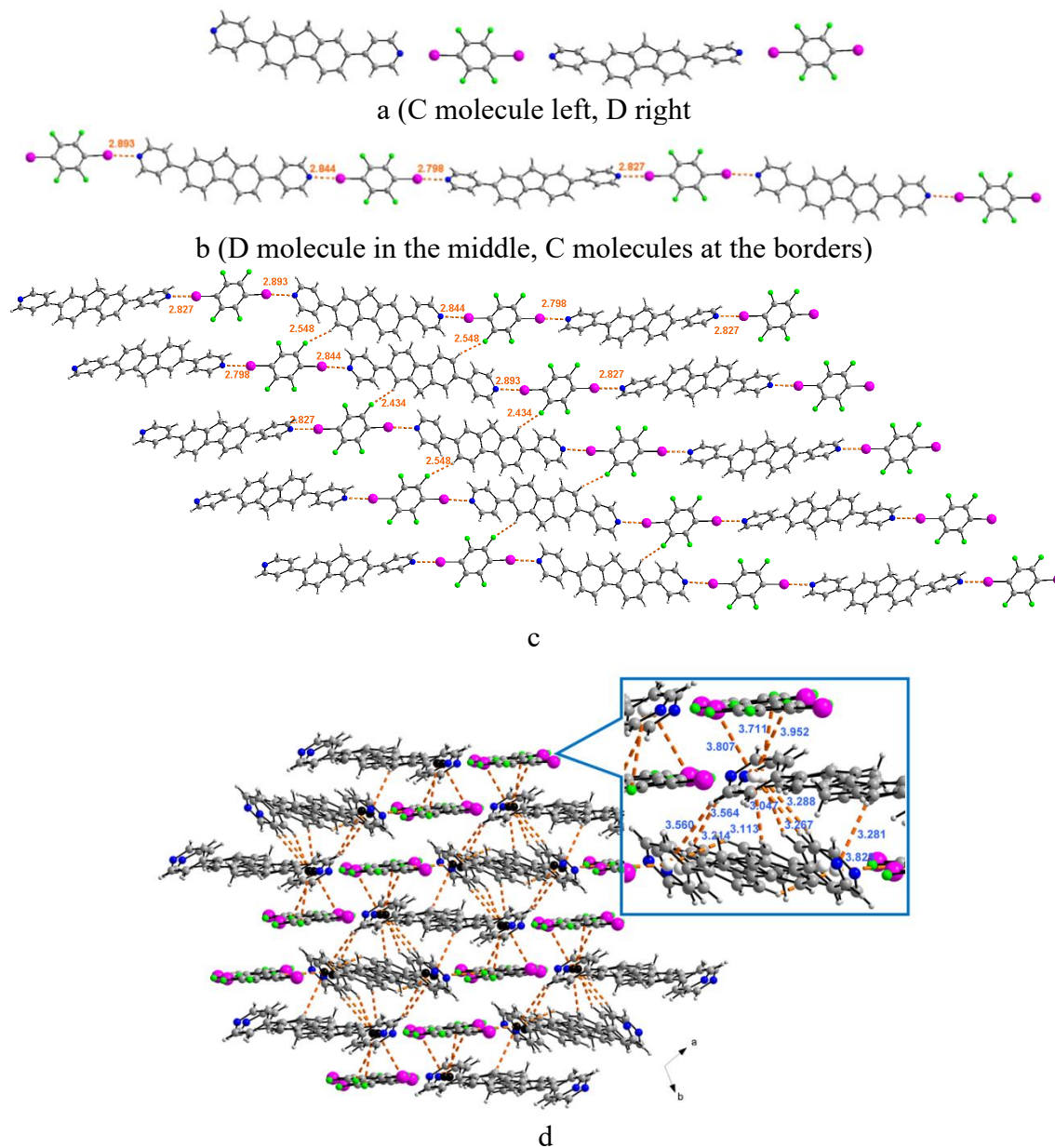


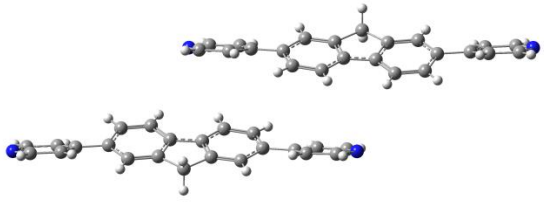
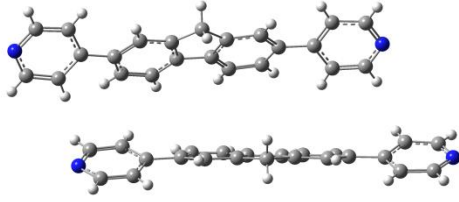
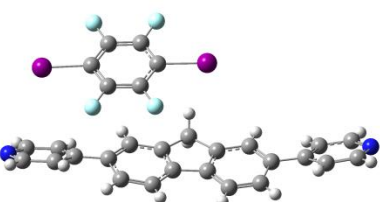
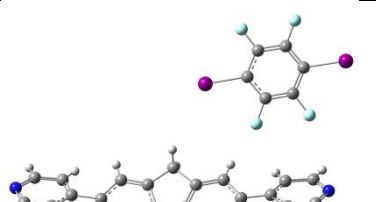
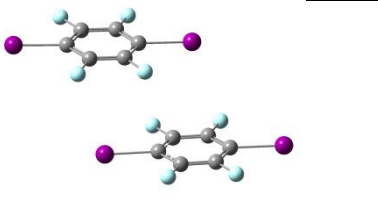
Figure 4. Single crystal X-ray structure of catemer **7**: repetitive unit (a); N---I catemer (b), 2D units (c) and 3D structure (d)

These parallel chains form a 2D layered structure and are interconnected (Figure 4c) one to each other via C(2'')-F---H-C(1) and C(2'')-F---H-C(3) interactions ( $d_{F\cdots H} = 2.434$  and  $2.548$  Å, respectively). The consecutive fluorene units (belonging to C and D units of 2,7-DPF) of the chains are located in two groups of parallel planes (the dihedral angle between the planes of different groups is  $39.1^\circ$  and in each group the fluorene moieties are oriented head to tail). The 2D layered units are close one to each other ( $d \approx 3$  Å) and they are connected (to form a 3D structure) via C(2'')-F---aromatic contacts [ $d_{F\text{-centroid Py}} = 3.712, 3.829, 3.951$  Å], I---aromatic [ $d_{I\text{-centroid Py}} = 3.807$  Å] and C-H---aromatic (Py) contacts [ $d_{C\text{-H---centroid Py}} = 3.047, 3.113, 3.214, 3.281, 3.288, 3.267, 3.560$  and  $3.564$  Å] (Figure 4d).

The theoretical calculations in case of **7** (Figure 5), besides the contributions of N---I halogen bonds ( $-7.01$  kcal/mol) revealed two types of 2,7-DPF dimer entities (stacked: Figure 5a and T-shaped: Figure 5b) which exhibit important contributions. The stabilization brought by T shaped dimer (estimated at  $-12.24$  kcal/mol) is higher than that calculated for the stacked dimer ( $-8.44$  kcal/mol). Two arrangements forming mixed pairs of 2,7-DPF and DITFB molecules were also observed. The stacking structures (Figure 5c;  $-9.31$ , kcal/mol) are strongly stabilized, while the T-shaped arrangements (Figure 5d) exhibit a weak contribution ( $-2.41$  kcal/mol) to the stabilization of the supramolecular architectures.

The close *p*-DITFB molecules in **7** are parallel and exhibit shifted *face-to-face* arrangements (Figure 5e) with quite reduced contribution ( $\Delta G^\circ = -4.46$  kcal/mol)

Stacking dimer with C and D 2,7-DPF units (a)	T shaped dimer with C and D 2,7-DPF units (b)
---	---

			
-8.44 kcal/mol		-12.24 kcal/mol	
<i>p</i> -DITFB-2,7-DPF stacking (c)	<i>p</i> -DITFB-2,7-DPF T shape (d)	<i>p</i> -DITFB - <i>p</i> -DITFB stacking (e)	
			
-9.31 kcal/mol	-2.41 kcal/mol	-4.46 kcal/mol	
Figure 5. Results of theoretical calculations for <b>7</b> ( $\Delta G^\circ$ )			

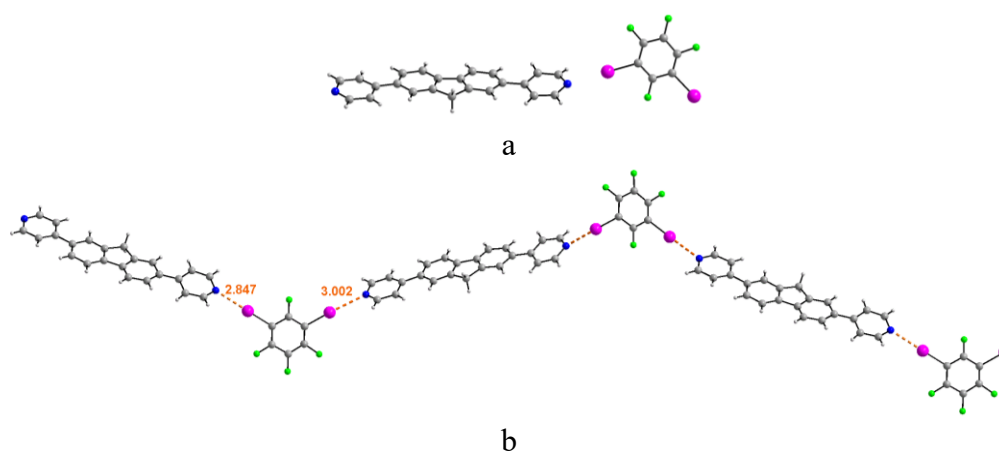
Theoretical calculations for **6** and **7** revealed in addition to the halogen-bonds the important contributions of the contacts between the aromatic units (2,7-DPF) and of the stacking of *p*-DIB or *p*-DITFB with 2,7-DPF molecules or among them.

The linear structures of polymers of **6** and **7** exhibit a light sinuosity due to the non-perfect linearity of the halogen acceptor (2,7-DPF molecules, see Chart 2). Non perfect linearity of the polymeric chains due to the structural particularities of halogen acceptors are encountered in literature and were observed in the single crystal X-ray diffraction structures of other supramolecular polymers of 1,4-DITFB with some specific bidentated acceptors as *trans*-1,2-dipyridylethene, [22, 23] 1-X,4-Y-cyclohexanes (X = Y or X  $\neq$  Y; X, Y = S, N, O) or DABCO [13, 24]. The high ability of *p*-DITFB to form linear catemers is also observed in their cocrystals with some peculiar acceptors

which can form bifurcated halogen bonds (e.g. 1,10-phenantroline-5,6-dione, [25], 2,2'-bipyrimidyl derivatives [25] or some acetylacetonates [26] complexes).

In the case of catemer **8**, the 2,7-DPF molecules exhibit planar fluorene moieties (Figure 6a) and slight torsions of pyridine rings ( $\beta, \gamma = 0.5$  and  $7.3^\circ$ ). Zigzag shaped chains (Figure 6b) are formed via N---I halogen bonds ( $d_{N\cdots I} = 3.002; 2.847 \text{ \AA}$ ). Parallel chains are connected (Figure 4c) via C(4'')-F---I ( $d_{I\cdots F} = 3.387 \text{ \AA}$ ) contacts and form 2D structures (sinuous (~~waved~~) layers, Figure 6c). The fluorene moieties of close parallel chains of the 2D structure are connected by C(9)-H---aromatic interactions [ $d_{C(9)\cdots H\cdots \text{centroid benzene}} = 3.293 \text{ \AA}$ ]. The consecutive *meta*-DITFB molecules of the chains are located in two sets of parallel planes (the angles among these planes is  $29.9^\circ$ ). In the chains, each molecule of *meta*-DITFB is parallel with its neighbors of every two layers. The lattice is formed by several sinuous parallel layers (the approximate distance between the layers is ~~around~~  $3 \text{ \AA}$ ).

The different layers are connected by C-H---aromatic [ $d_{C(4)\cdots H\cdots \text{centroid pyridine}} = 2.817; d_{C(1)\cdots H\cdots \text{centroid pyridine}} = 3.377 \text{ \AA}$ ] and C(9)-H---I ( $d = 3.016 \text{ \AA}$ ) contacts (Figure 6d).





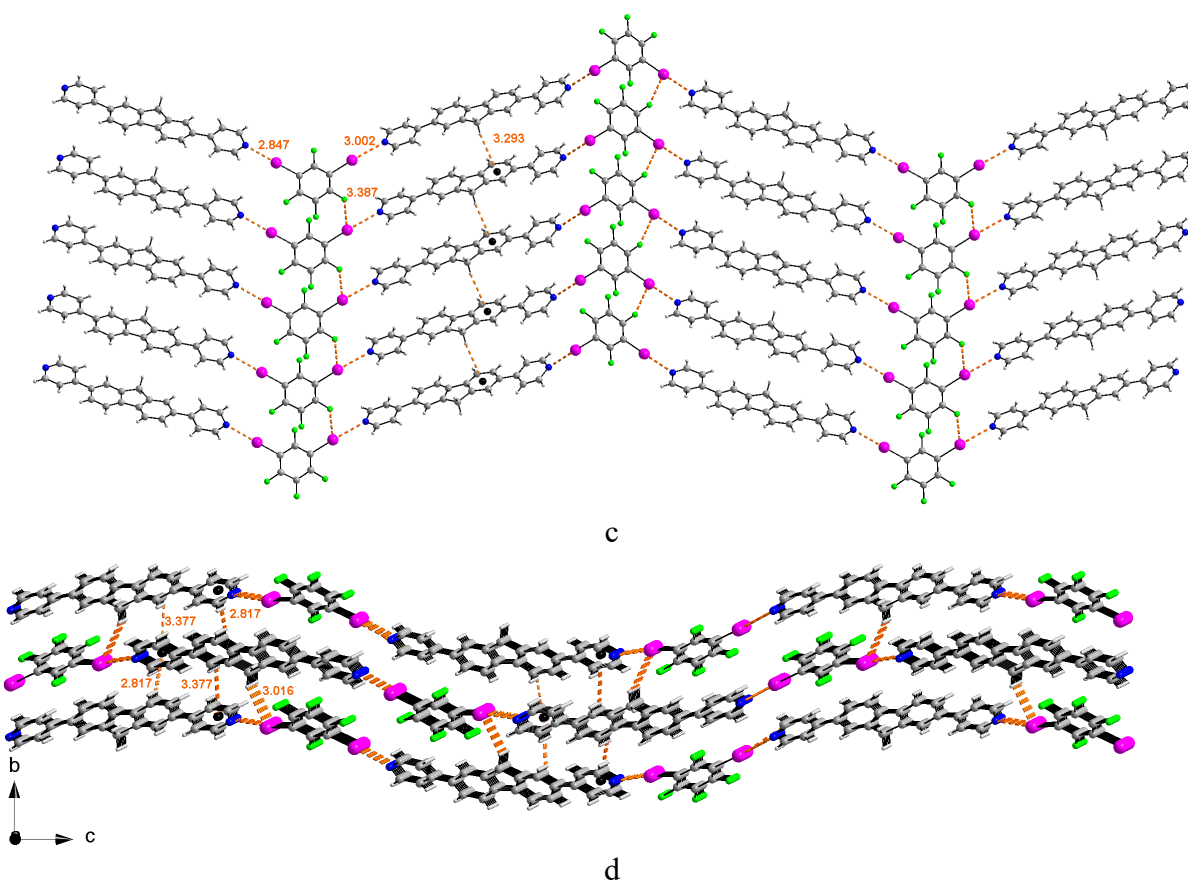
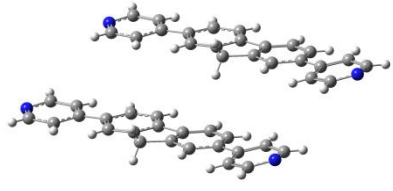
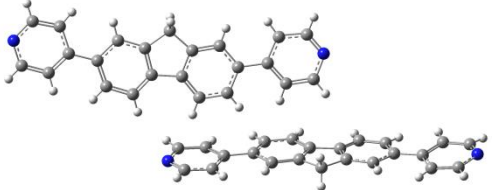
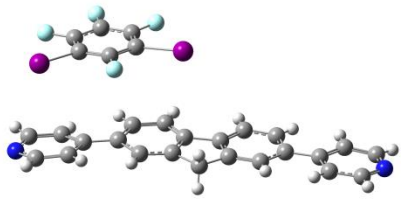
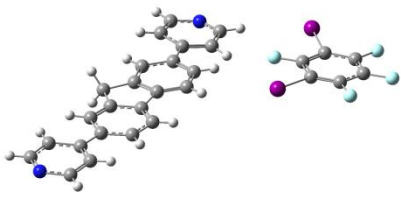
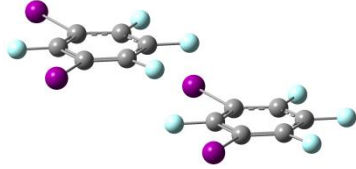


Figure 6. Single crystal X-ray structure of catemer **8**: repetitive unit (a); N...I catemer (b), 2D units (c) and 3D structure (d)

Besides the contributions of N...I halogen bonds (-5.69 kcal/mol) for **8**, theoretical calculations revealed two types of 2,7-DPF dimer entities [stacked: Figure 7a  $\Delta G^\circ = -8.89$  kcal/mol and T-shaped: Figure 7b,  $\Delta G^\circ = -7.35$  kcal/mol] which exhibit important contributions. The stabilization of the solid state structure brought by these two 2,7-DPF dimers are close to that determined for the stacked 1,3-DITBF / 2,7-DPF molecules (Figure 7c; -8.97 kcal/mol). For the other two stacking units of 1,3-DITFB-2,7-DPF (Figure 7d, *in plane*) and 1,3-DITFB-1,3-DITFB (Figure 7e, shifted *face-to-face* with antiparallel orientations) the calculated stabilization energies are considerably lower (-2.24 and -2.57 kcal/mol, respectively)

Stacking dimer with 2,7-DPF units (a)	T shaped dimer units (b)
---------------------------------------	--------------------------



		
-8.89 kcal/mol	-7.35 kcal/mol	
<i>m</i> -DITFB-2,7-DPF T shaped dimer (c)	<i>m</i> -DITFB-2,7-DPF “in plane” stacking (d)	<i>m</i> -DITFB - <i>m</i> -DITFB stacking (e)
		
-8.97 kcal/mol	-2.24 kcal/mol	-2.57 kcal/mol
Figure 7. Results of theoretical calculations for <b>8</b> ( $\Delta G^\circ$ )		

The repetitive unit of catemer **9** exhibits three types of 2,7-DPF and *ortho*-DITFB molecules (Figure 8, a). The 2,7-DPF molecules show different torsion angles ( $\beta$ ,  $\gamma$ ) of the pyridine rings with the fluorene core (E = 16.2, 24.2 °; F = 14.9, 24.5 °; G= 24.1, 27.5°).

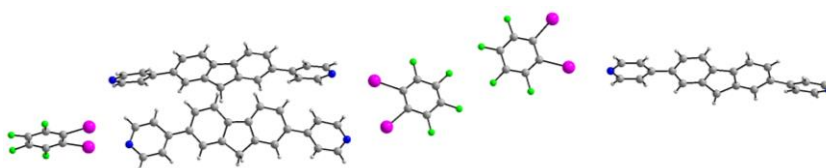
The main interactions in the supramolecular polymer are given by N---I contacts (the distances are different for each type of 2,7-DPF; E ( $d_{N---I}$  = 3.286; 2.914 Å); F ( $d_{N---I}$  = 3.065; 2.989 Å) and G ( $d_{N---I}$  = 3.042; 2.980 Å). Some of the iodine atoms [with longer N---I ( $d > 3\text{Å}$ ) contacts] exhibit also I---H-C(2') interactions [ $d_{I---H}$  = 3.041 and 3.385 for F molecules]

There are two types of similar sinusoidal chains [E(2,7-DPF)-*o*-DITFB] $_n$  [noted as ( $W_E$ ) $_n$  Figure 8, b] and [F(2,7-DPF)-*o*-DITFB-G(2,7-DPF)-*o*-DITFB] $_p$  [noted as ( $W_{FG}$ ) $_p$ ;  $n = 2p$ ] Figure 8, c] described by the N---I halogen bonds. ( $W_E$ ) $_n$  involves only 2,7-DPF units of type E, while in the other catemeric chain the alternative presence of units of types F and G are observed. The aromatic parts of columns ( $W_E$ ) $_n$  are connected by C(4)-H---benzene contacts [ $d_{C(4)-H---\text{centroid}}$  = 3.128

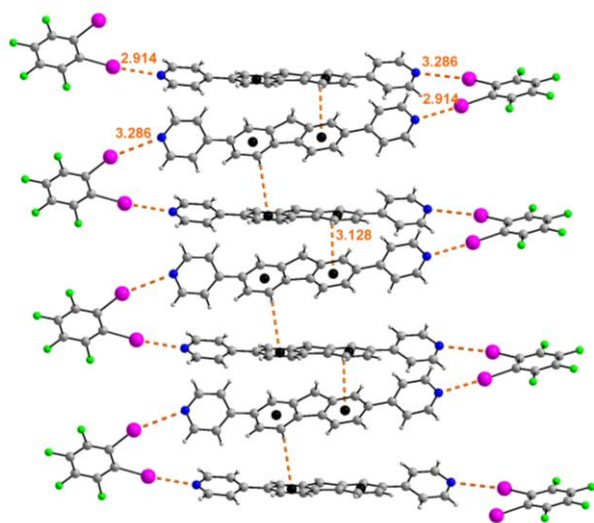
Å. The *o*-DITFB units of column  $(W_E)_n$  are located in two sets of parallel planes (the dihedral angle between the planes is  $71.7^\circ$ ). The consecutive 2,7-DPF units are also twisted and they are also located in two sets of parallel planes (the dihedral angle between the planes of consecutive fluorene moieties is  $48.8^\circ$ ). The 2,7-DPF entities of columns  $(W_{FG})_p$  are connected by C(9)-H---centroid benzene ( $d = 3.230 \text{ \AA}$ ), C(4)-H---centroid benzene ( $d = 2.981 \text{ \AA}$ ), C(5)-H---centroid benzene ( $d = 3.214 \text{ \AA}$ ), and C(3')-H---centroid pyridine ( $d = 3.085, 3.226 \text{ \AA}$ ) and C(2')-H---centroid pyridine ( $d = 3.270 \text{ and } 3.225 \text{ \AA}$ ) contacts. The dihedral angle between the planes of consecutive *o*-DITFB molecules is  $89.5^\circ$ , while the fluorene units of neighboring 2,7-DPF molecules show a dihedral angle of  $53.1^\circ$ .

The  $(W_E)_n$  columns are connected ones to each others by I---F contacts [ $d \text{ C}(3'')\text{-F---I} = 3.424 \text{ \AA}$ ], and form 2D sheets (Figure 8, d and e).

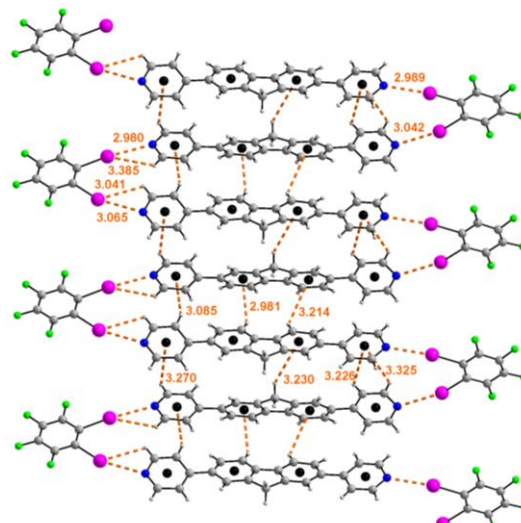
$(W_{FG})_p$  columns are also connected ones to each others in a similar way as the  $(W_E)_n$  ones giving specific 2D structures (Figure 8, f and g). The I---F [ $d \text{ C}(3'')\text{-F---I} = 3.366 \text{ and } 3.423 \text{ \AA}$ ] and some I---aromatic [ $d \text{ I---centroid DITFB} = 4.001 \text{ and } 4.010 \text{ \AA}$ ] are involved in the formation of the layers in this case (Figure 5, g). In the lattice two  $[(W_{FG})_p]_m$  sheets are connected one to the other (Figure 8, h: in the top the green and the red sheets).



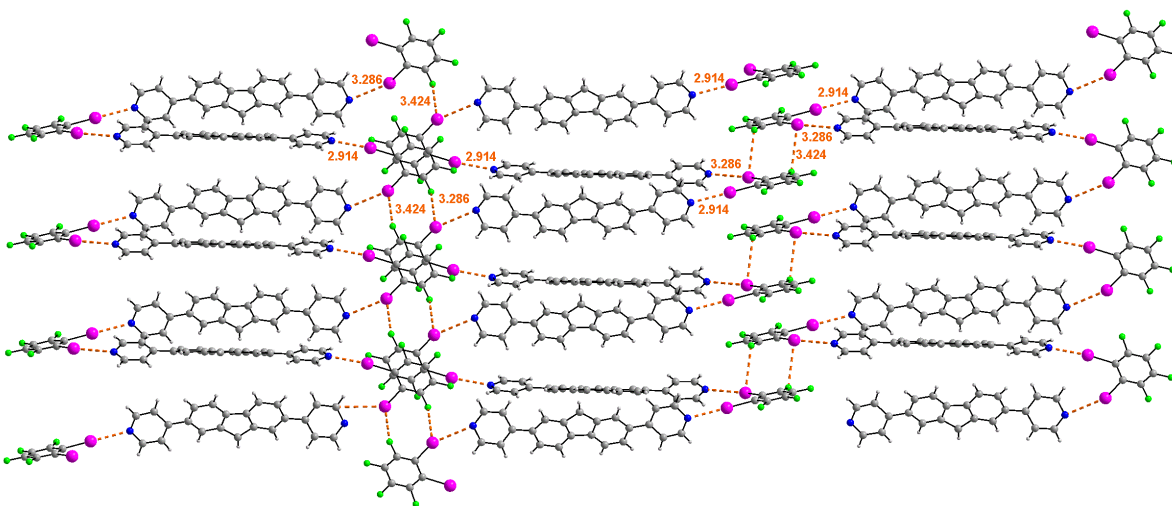
a (F: left bottom, G: left above and E: right)



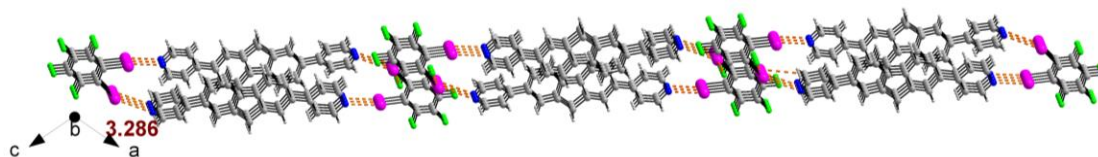
b



c



d



e

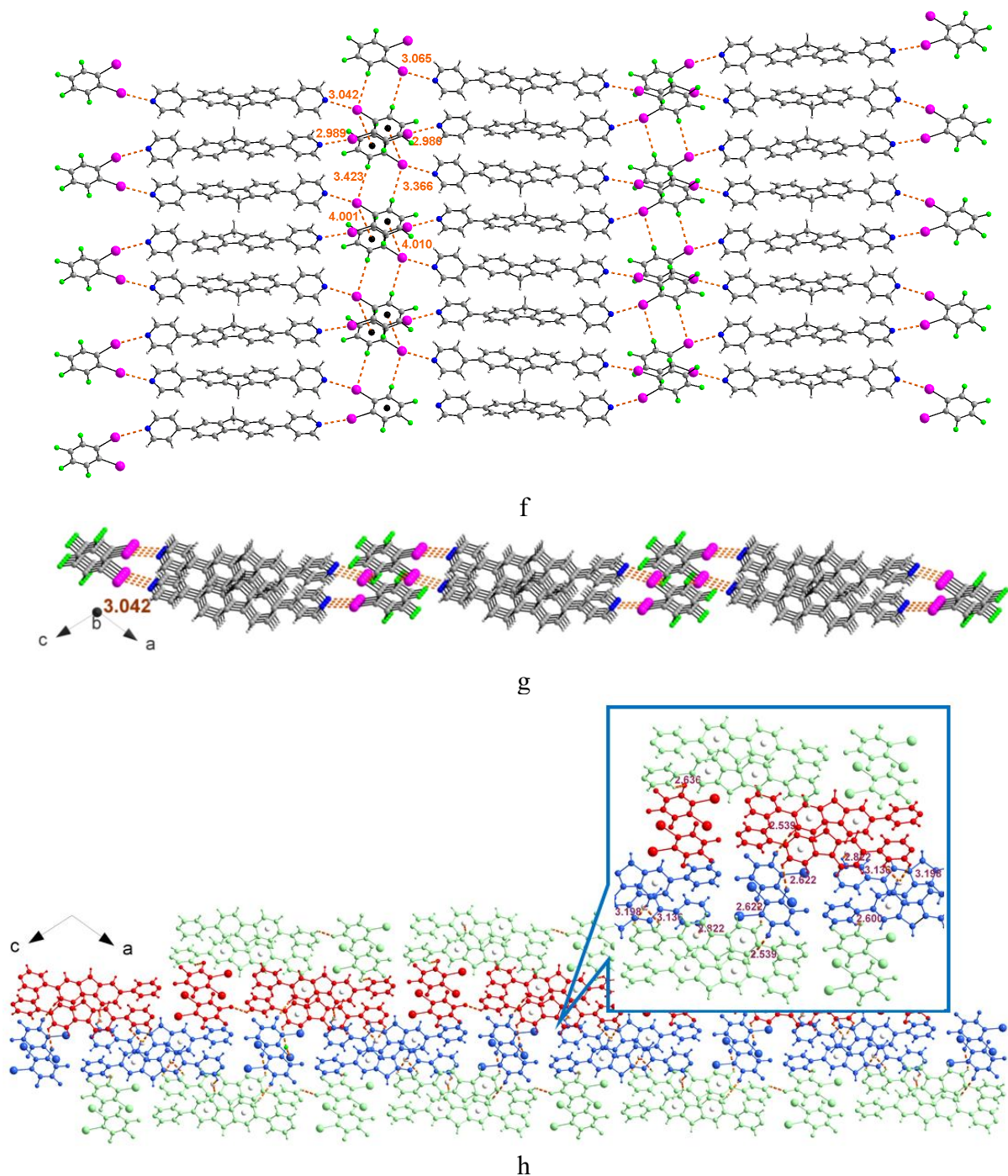


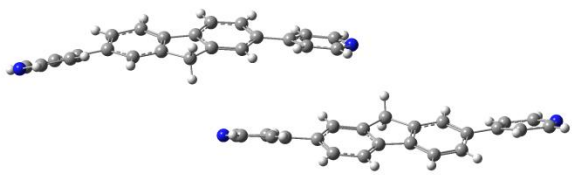
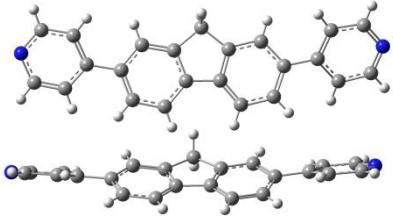
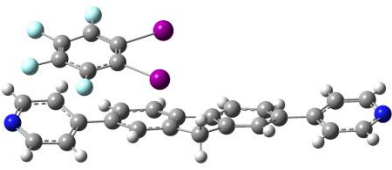
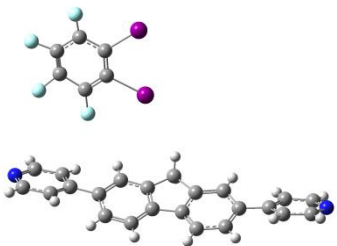
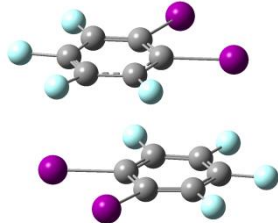
Figure 8. Single crystal X-ray structure of catemer **9**: repetitive unit (a);  $(W_E)_n$  column (b);  $(W_{FG})_p$  column (c); sheet with  $(W_E)_n$  columns [view along a (d) and b (e) crystallographic axes]; sheet with  $(W_{FG})_p$  columns [view along a (f) and b (g) crystallographic axes] and 3D structure with  $-(W_{FG})_p$ - $[(W_{FG})_p]_m$ - $[(W_E)_n]_m$ - $[(W_{FG})_p]_m$ -arrangement of the layers (h)

The connections of  $[(W_{FG})_p]_m$  layers is reinforced via  $C(3'')-F---H-C(3') = 2.636 \text{ \AA}$  contacts. The two assembled  $[(W_{FG})_p]_m$  sheets are connected on the free faces with  $[(W_E)_n]_m$  sheets. A formation

of four sheets  $-(W_{FG})_p-(W_{FG})_p-(W_E)_n-(W_{FG})_p-$  is shown in figure 8 {h,  $[(W_E)_n]_m$  is depicted in blue, while the  $[(W_{FG})_p]_m$  sheets are depicted in red and green}, The structure of the crystal is described by the formula  $-{[(W_E)_n]_m-[(W_{FG})_p]_m-[(W_{FG})_p]_m}_z-$  ( $n = 2p$ ). The connection of the different sheets are due to C-F---H-C contacts { $dC(3'')-F---H-C(3')(F) = 2.539 \text{ \AA}$ ;  $dC(3'')-F---H-C(3)(G) = 2.622 \text{ \AA}$ ;  $dC(3'')-F---H-C(3)(E) = 2.600 \text{ \AA}$ } and C-H---aromatic contacts [ $C(2')-H(E)-$ --benzene centroid (G) =  $2.822 \text{ \AA}$  and  $dC(3')-H---$ centroid benzene =  $3.136, 3.198 \text{ \AA}$ .

According to theoretical calculations, the contributions of N---I halogen bonds for **9** (-4.80 kcal/mol) are lower than for **7** and **8** (**7**: -7.01, **8**: -5.69 kcal/mol) but the contacts observed in other molecular arrangements of the lattice (Figures 9a-e) participate to the stabilization of the structure. The stacked and the T-shaped dimeric structures of 2,7-DPF molecules (Figure 9a and 9b) bring a lowering of the energy in the lattice of  $\Delta G^\circ = -6.25$  and  $-11.78$  kcal/mol, respectively. The stabilization observed by the associations of 1,2-DITFB and 2,7-DPF molecules in the parallel and T-shaped structures (Figures 9c and 9d) is of  $\Delta G^\circ = -10.24$  and  $-2.35$  kcal/mol, respectively, while the antiparallel stacked arrangement of two 1,2-DITFB molecules (Figure 9e) reveal the highest interactions of this type in the series of **7** – **9** being important with a value of  $\Delta G^\circ = -8.31$  kcal/mol [for comparison, these interactions are weak in **8** ( $\Delta G^\circ = -2.57$  kcal/mol) and moderate in **7** ( $\Delta G^\circ = -4.46$  kcal/mol)]. These dimeric 1,2-DITFB units are important and they rely the different columns (zigzag chains) into a 2D structure.

Stacking dimer with 2,7-DPF units (a)	T shaped dimer with 2,7-DPF units (b)
---------------------------------------	---------------------------------------

			
-6.25 kcal/mol		-11.78 kcal/mol	
<i>o</i> -DITFB-2,7-DPF stacking (c)	<i>o</i> -DITFB-2,7-DPF T shape (d)	<i>o</i> -DITFB - <i>o</i> -DITFB stacking (e)	
			
-10.24 kcal/mol	-2.35 kcal/mol	-8.31 kcal/mol	
Figure 9. Results of theoretical calculations for <b>9</b> ( $\Delta G^\circ$ )			

Zigzag type catemers, similar to those of **8** and **9**, were also reported in the cocrystals of 1,3- and/or 1,2-DITFB with other halogen acceptors as [Cl<sup>-</sup>, [11, 12], aromatic heterocycles with two nitrogen atoms (e.g. 1,4-diazine, 1,4-diazanaphthalene or 9,10-diazaanthracene) [13]. The zigzag shape of the catemers could be also induced by the structure of the halogen acceptors and in this case such structures are obtained even when linear 1,4-DITFB is used as halogen donor. Relevant examples of zigzag chains were reported for the crystals of 1,4-DITFB with 1,4-bis(pyridine-3'-yl)-, 1,4-bis(quinoline-4'-yl)- and 1,4-bis(isoquinoline-4'-yl)-1,3-butadiyne, [22] and terpyridine (in *trans-trans* configuration) derivatives. [27] Tetraiodoethene and 2,3,5,6-tetrapyridylbenzene are leading to formally linear catemers by the formation of cyclic entities by N---I contacts. [28]

*Solid state FTIR and solution multinuclear NMR investigations*



The FT-IR spectra of halogen acceptor **1** and donors (**2**, **3** and **5**) were compared with the corresponding spectra of the co-crystals (**6-9**) in order to evaluate the presence of halogen bonding interactions. The observed shifts between the free and bound molecules, for some IR vibrational bands, are presented in **Table 2** and **Figure 10**. Similar to the literature [29], there is a shift of the band corresponding to the C=N bond (around 1600 cm<sup>-1</sup>) of **1**, but it is small for all investigated co-crystals. According to the literature [30], the band around 1300 cm<sup>-1</sup> was assigned to symmetric ring contraction of the halogen bonding donors. We have observed small shifts of the IR bands only for the two *para*-positioned donors (**2** and **3**). Some changes were also measured for vibrational bands between 1400 - 1500 cm<sup>-1</sup>, previously [30] associated with the C-C stretch vibration. The formation of halogen bonding generated some other small shifts in the band at 802 cm<sup>-1</sup> of the acceptor **1**, while in case of donor **3** we noticed two bands moving after the co-crystallization with the acceptor.

Table 2. Relevant data concerning the modification of IR bands in cocrystals **6-9** in comparison with the starting compounds **1-3** and **5**

Cmpd	IR vibration bands (cm <sup>-1</sup> )							
	C=N	C-C stretch			Ring contraction	Other vibrations		
<b>1</b>	1590	1411			-	802		
<b>2</b>					1370			
<b>3</b>			1467		1355		759	945
<b>5</b>			1442	1493				
<b>6</b>	1592	1409			1373	808		
<b>7</b>	1593	no shift	1455		1360		751	940
<b>8</b>	1591	no shift				807		
<b>9</b>	1592	no shift	1438	1485				

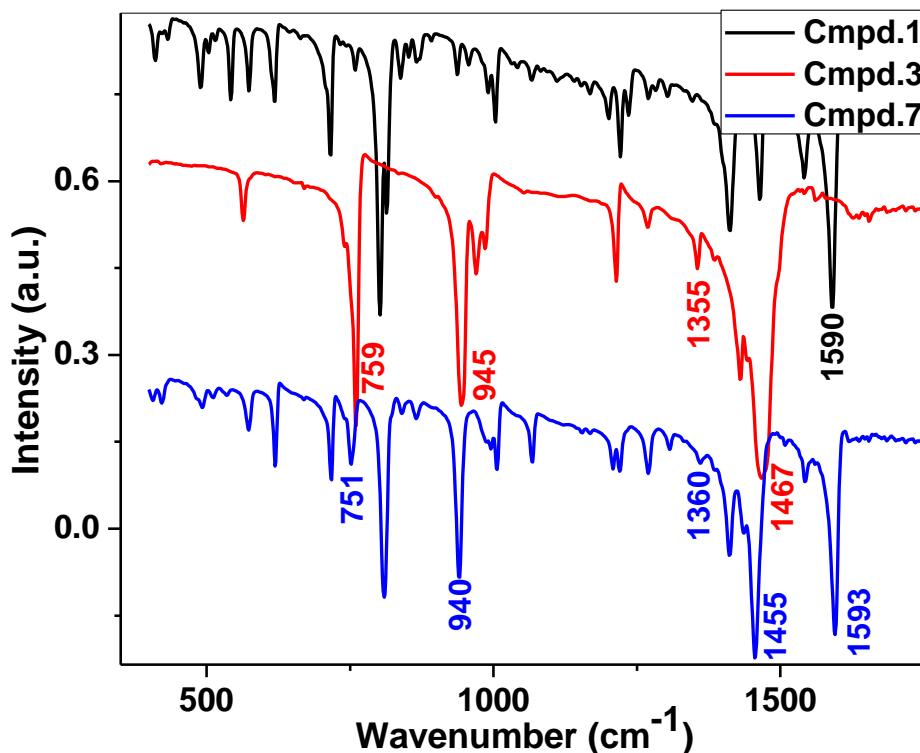


Figure 10. Comparison of FTIR spectra of **1**, **3** and **7**

The characterization of N---I halogen bonding by solving the corresponding cocrystals in chloroform solutions was attempted using NMR experiments. Thus,  $^1\text{H}$ -NMR,  $^{19}\text{F}$ -NMR and  $^1\text{H}$ ,  $^{15}\text{N}$ -HMBC spectra of ligand **1**, of diiodotetrafluorobenzene isomers **3-5** and of cocrystals **7-9** were recorded in order to observe  $^1\text{H}$ ,  $^{19}\text{F}$  and  $^{15}\text{N}$  NMR chemical shift changes as result of the halogen bonding associations (spectra are presented in SI). For the measurements of the NMR behavior of the associated molecules, the investigated solutions were obtained the NMR solvent.

The comparison of the spectra of free ligands and cocrystals in both  $^1\text{H}$  and  $^{19}\text{F}$  NMR experiments showed relevant shifting of the signals. Thus, the signals of the protons at positions 2' (close to N atom of pyridine rings) and 3' exhibiting  $\delta_{2'} = 8.705$  and  $\delta_{3'} = 7.698$  ppm in 2,7-DPF (**1**) were shifted in the spectra of **7-9** at  $\delta_{2'} = 8.691, 8.694$  and  $8.693$  ppm and  $\delta_{3'} = 7.601,$



7.622 and 7.616 ppm. The shifting (upfield) of the signals ( $\Delta\delta_2$ ) for the protons at positions 2' are - 0.014 (**7**), - 0.011 (**8**) and - 0.010 ppm (**9**), while for the signals belonging to the protons at positions 3' considerably higher shifts (upfield,  $\Delta\delta_3$ ) were observed [0.097 (**7**), 0.076 (**8**) and 0.082 (**9**) ppm]. The signals in  $^{19}\text{F}$  NMR spectra of **7-9** are all shifted in comparison with the signals recorded in the spectra of free diiodotetrafluorobenzene isomers **3-5** (*i.e.* for accuracy the chemical shifts were determined using hexafluorobenzene as external reference added in a closed capillary in the NMR tubes). In the spectrum of *p*-DITFB (**3**) there is one signal at  $\delta(^{19}\text{F}) = 119.102$  ppm and it is moved in the spectrum of **7** at  $\delta(^{19}\text{F}) = 119.093$  ppm ( $\Delta\delta = - 0.009$  ppm). The spectra of *m*-DITFB (**4**) and *o*-DITFB (**5**) exhibits three [**4**:  $\delta(^{19}\text{F}) = 77.319, 111.544$  and  $159.142$  ppm] and two signals [**5**:  $\delta(^{19}\text{F}) = 105.553$  and  $152.486$  ppm] which are significantly shifted in the spectra of **8** [ $\delta(^{19}\text{F}) = 77.541, 111.658$  and  $159.281$  ppm] and **9** [ $\delta(^{19}\text{F}) = 105.049$  and  $152.905$  ppm] being recorded  $\Delta\delta$  values of 0.142, 0.114 and 0.139 ppm for **4 / 8** and of - 0.504 and 0.419 ppm for **5 / 9** comparisons.

Direct evidences for the formation of X---N halogen-bond in solution were obtained by observing the  $^{15}\text{N}$  chemical shifts changes in the spectra of **7-9** and **1**.  $^{15}\text{N}$ -chemical shifts were indirectly determined from  $^1\text{H},^{15}\text{N}$  HMBC spectra through the correlation between pyridine nitrogen and the proton located at the carbon in  $\beta$ -position. In order to increase the resolution and accuracy,  $^{15}\text{N}$  was referenced to quinoline used as external standard, added in a closed capillary in the NMR tube (*i.e.* the chemical shift of quinoline nitrogen was determined at -68.18 ppm using nitromethane as internal standard), and the spectral window for  $^{15}\text{N}$  spectrum was set to 60 ppm, following a previously reported protocol. [31] Small variations in the chemical shifts of  $^{15}\text{N}$  for the cocrystals of **1** with *ortho*-, *meta*- and *para*-diiodotetrafluorobenzene at  $\delta(^{15}\text{N}) = -70.54$  ppm, -70.96 ppm and -70.27 ppm, respectively, were observed. Unfortunately,  $\delta(^{15}\text{N})$  for the nitrogen

atom in ligand **1** could not be determined due to the low solubility of quinoline. However, the small changes in  $^{15}\text{N}$  chemical shifts of pyridine nitrogen in the spectra of **7-9**, together with the relevant shifting of the signals in  $^1\text{H}$  and  $^{19}\text{F}$  NMR spectra in cocrystals can be considered as evidences for the presence of I---N halogen bond associations in solution, too.

## Conclusions

~~The single crystal X-ray diffraction structures of catemeric supramolecular architectures obtained by the cocrystallization of 2,7-dipyridylfluorene with the isomers of diiodotetrafluorobenzene and with *para*-diiodobenzene revealed the formation of catemeric structures via N---I halogen bonds and further organization of the catemers into 3D networks reinforced by other contacts (C---H---aromatic, C---H---F, F---I). The theoretical calculations revealed the important role of the contacts between the aromatic units of 2,7-dipyridylfluorene molecules for the crystal cohesive energy. The shape of the structures is strongly correlated with *para*, *meta* or *ortho* position of the iodine atoms and the N---I halogen bonding are considerably stronger in the tetrafluoro derivatives as compared to the simple *para*-diiodobenzene as supported by observed bonding distances and confirmed by theoretical calculations~~

The single crystal X-ray diffraction structures of supramolecular architectures obtained by the cocrystallization of 2,7-dipyridylfluorene with the isomers of diiodotetrafluorobenzene and with *para*-diiodobenzene revealed the formation, via N---I halogen bonds, of linear catemers in the cases of *para*-diiodobenzene compounds and zigzag catemers for *meta*- and *ortho*- isomers of DITFB. The N---I contacts are weaker for the non-fluorinated diiodobenzene halogen donor and considerably stronger for the diiodotetrafluorinated halogen donors, decreasing in the series *para* > *meta* > *ortho* as it can be deduced from bonding distances and theoretical calculations. The

organization of the catemers into 3D networks is reinforced by other contacts (C-H---aromatic, C-H---F, F---I). The contacts in dimer 2,7-DPF entities, either in stacked (**6**, **7** and **8**) or in T shaped (**8** and **9**) arrangements play an important role for the crystal cohesive energy, while the stacking among DITFB molecules has an important role for **9**.

## Acknowledgements

We are grateful for the financial support of this work by CNCS-UEFISCDI, project PN-III-P4-ID-PCCF-2016-0088 and by the Ministry of Research and Innovation—MCI, Core Programme, Projects PN19 35 02 01 and PNCDI III 32 PFE.

## References

- [1] a) Lehn, J.-M. *Supramolecular chemistry: concepts and perspectives*; VCH, Weinheim, **1995**; b) Steed, J. W.; Atwood, J. L. *Supramolecular Chemistry*, Wiley, New York, **2009**; c) Bårboiu, M. *Constitutional Dynamic Chemistry*, Springer-Verlag, Berlin, **2011**; d) Lehn, J.-M., *Angew. Chem. Int. Ed.* **2015**, *54*, 3276 – 3289; e) Amabilino, D. B.; Smith, D. K.; Steed, J. W., *Chem. Soc. Rev.* **2017**, *46*, 2404-2420.
- [2] a) Adachi, T.; Ward, M. D., *Acc. Chem. Res.* **2016**, *49*, 2669-2679; b) Mahmudov, K. T.; Pombeiro, A. J. L., *Chem. Eur. J.* **2016**, *22*, 16356 – 16398; c) Takahashi, O.; Kohno, Y.; Nishio, M., *Chem. Rev.* **2010**, *110*, 6049–6076; d) Montoro-García, C.; Camacho-García, J.; López-Pérez, A. M.; Mayoral, M. J.; Bilbao, N.; González-Rodríguez, D., *Angew. Chem. Int. Ed.* **2016**, *55*, 223 – 227; e) Prins, L. J.; Reinhoudt, D. N.; Timmerman, P., *Angew. Chem. Int. Ed.* **2001**, *40*, 2382 – 2426; f) Pop, L.; Hadade, N. D.; van der Lee, A.; Barboiu, M.; Grosu, I.; Legrand, Y.-M., *Cryst. Growth Des.* **2016**, *16*, 3271–3278; g) Circu, M.; Pascanu, V.; Soran, A.; Braun, B.; Terec, A.; Socaci, C.; Grosu, I., *CrystEngComm* **2012**, *14*, 632-639.
- [3] a) Hwang, J.; Li, P.; Shimizu, K. D., *Org. Biomol. Chem.* **2017**, *15*, 1554–1564; b) Das, A.; Ghosh, S., *Angew. Chem. Int. Ed.* **2014**, *53*, 2038 – 2054.
- [4] a) Biedermann, F.; Nau, W. M.; Schneider, H.-J., *Angew. Chem. Int. Ed.* **2014**, *53*, 11158 – 11171; b) Jordan, J. H.; Gibb, B. C., *Chem. Soc. Rev.* **2015**, *44*, 547-585; c) Pop, L.; Dumitru, F.; Hādade, N. D.; Legrand, Y.-M.; van der Lee, A.; Barboiu, M.; Grosu, I., *Org. Lett.* **2015**, *17*, 3494-3497.
- [5] a) Takemura, A.; McAllister, L. J.; Hart, S.; Pridmore, N. E.; Karadakov, P. B.; Whitwood, A. C.; Bruce, D. W. *Chem. Eur. J.* **2014**, *20*, 6721-6732; b) Szell, P. M. J.; Zablotny, S.; Bryce, D. L. *Nat. Commun.* **2019**, Article number: 916; c) Caballero, A.; Zapata, F.; White, N. G.; Costa, P. J.; Félix, V.; Beer, P. D., *Angew. Chem. Int. Ed.* **2012**, *51*, 1876 – 1880; d) Widner, D. L.; Knauf, Q. R.; Merucci, M. T.; Fritz, T. R.; Sauer, J. S.; Speetzen, E. D.; Bosch, E.; Bowling, N. P., *J. Org.*

*Chem.* **2014**, *79*, 6269–6278; e) Ding, X.; Tuikka, M.; Haukka, M.; *Halogen Bonding in Crystal Engineering* (book chapter) in *Recent Advances in Crystallography* (Benedict, J. B., editor), IntechOpen, **2012**, DOI: 10.5772/48592; f) Rednic, M. I.; Varga, R. A.; Bende, A.; Grosu, I. G.; Miclăuş, M.; Hădade, N. D.; Terec, A.; Bogdan, E.; Grosu, I., *Chem. Commun.*, **2016**, *52*, 12322–12325; g) Grosu, I. G.; Rednic, M. I.; Miclăuş, M.; Grosu, I.; Bende, A., *Phys. Chem. Chem. Phys.* **2017**, *19*, 20691–20698.

[6] a) Li, S.-L.; Xiao, T.; Lin, C.; Wang, L., *Chem. Soc. Rev.* **2012**, *41*, 5950–5968; b) Liu, R.; Wang, H.; Jin, W. J., *Cryst. Growth Des.* **2017**, *17*, 3331–3337; b) von Krbek, L. K. S.; Schalley, C. A.; Thordarson, P., *Chem. Soc. Rev.* **2017**, *46*, 2622–2637; c) Saha, M. L.; De, S.; Pramanik, S.; Schmittel, M., *Chem. Soc. Rev.* **2013**, *42*, 6860 – 6909; d) Hu, X.-Y.; Xiao, T.; Lin, C.; Huang, F.; Wang, L., *Acc. Chem. Res.* **2014**, *47*, 2041–2051; e) He, Z.; Jiang, W.; Schalley, C. A., *Chem. Soc. Rev.* **2015**, *44*, 779–789

[7] a) Mingos, D. M. P.; Series Editor for *Structure and Bonding*, Metrangolo, P.; Resnati, G.; editors for volume 126: *Halogen Bonding – Fundamentals and Applications*, Springer, Berlin, **2008**; b) Metrangolo, P.; Resnati, G.; editors, *Halogen Bonding II, Impact on the Materials Chemistry and Life Sciences, Topics in Current Chemistry*, Springer, Berlin, **2015**, volume 359; d) Aakeröy, C. B.; Baldrighi, M.; Desper, J.; Metrangolo, P.; Resnati, G., *Chem. Eur. J.* **2013**, *19*, 16240 – 16247; e) Cavallo, G.; Metrangolo, P.; Milani, R.; Pilati, T.; Priimagi, A.; Resnati, G.; Terraneo, G., *Chem. Rev.* **2016**, *116*, 2478–2601; f) Bulfield, D.; Huber, S. M., *Chem. Eur. J.* **2016**, *22*, 14434 – 14450; g) Priimagi, A.; Cavallo, G.; Metrangolo, P.; Resnati, G., *Acc. Chem. Res.* **2013**, *46*, 2686 – 2695.

[8] a) Ng, C.-F.; Chow, H.-F.; Mak, T. C. W., *Angew. Chem. Int. Ed.* **2018**, *57*, 4986–4990; b) Turunen, L.; Warzok, U.; Puttreddy, R.; Beyeh, N. K.; Schalley, C. A.; Rissanen, K. *Angew. Chem. Int. Ed.* **2016**, *55*, 14033–14036; c) Sinnwell, M. A.; MacGillivray, L. R., *Angew. Chem. Int. Ed.* **2016**, *55*, 3477–3480; c) Dumele, O.; Schreib, B.; Warzok, U.; Trapp, N.; Schalley, C. A.; Diederich, F., *Angew. Chem. Int. Ed.* **2017**, *56*, 1152–1157; d) Jungbauer, S. H.; Bulfield, D.; Kniep, F.; Lehmann, C. W.; Herdtweck, E.; Huber, S. M., *J. Am. Chem. Soc.* **2014**, *136*, 16740–16743;

[9] a) Liu, P.; Li, Z.; Shi, B.; Liu, J.; Zhu, H.; Huang, F. *Chem. Eur. J.* **2018**, *24*, 4264–4267; b) Yan, D.; Delori, A.; Lloyd, G. O.; Frišćić, T.; Day, G. M.; Jones, W.; Lu, J.; Wei, M.; Evans, D. G.; Duan, X., *Angew. Chem. Int. Ed.* **2011**, *50*, 12483–12486.

[10] a) Dumele, O.; Wu, D.; Trapp, N.; Goroff, N.; Diederich, F. *Org. Lett.*, **2014**, *16*, 4722–4725; b) Maugeri, L.; Asencio-Hernández, J.; Lébl, T.; Cordes, D. B.; Slawin, A. M. Z.; Delsuc, M.-A.; Philp, D., *Chem. Sci.*, **2016**, *7*, 6422–6428; c) Erdélyi, M. *Chem. Soc. Rev.*, **2012**, *41*, 3547–3557.

[11] Pfrunder, M. C.; Micallef, A. S.; Rintoul, L.; Arnold, D. P.; Davy, K. J. P.; McMurtrie, *Cryst. Growth Des.*, **2012**, *12*, 714–724.

[12] Pfrunder, M. C.; Micallef, A. S.; Rintoul, L.; Arnold, D. P.; Davy, K. J. P.; McMurtrie, *Cryst. Growth Des.*, **2014**, *14*, 6041–6047.

[13] Bedeković, N.; Stilinović, V.; Frišćić, T.; Cinčić, D., *New J. Chem.* **2018**, *42*, 10584–10591.

- [14] a) Howard, J. L.; Cao, Q.; Browne, D. L., *Chem. Sci.* **2018**, *9*, 3080-3094; b) Leonardi, M.; Villacampa, M.; Menéndez, J. C., *Chem. Sci.* **2018**, *9*, 2042-2064; c) Obst, M.; König, B., *Eur. J. Org. Chem.* **2018**, 4213–4232;
- [15] Schütz, M.; Hetzer, G.; Werner, H.-J., *J. Chem. Phys.* **1999**, *111*, 5691-5705.
- [16] Werner, H.-J.; Manby, F. R.; Knowles, P. J., *J. Chem. Phys.* **2003**, *118*, 8149-8160.
- [17] Werner, H.-J.; Knowles, P. J.; Knizia, G.; Manby F. R.; Schütz, M., *WIREs Comput. Mol. Sci.* **2012**, *2*, 242-253.
- [18] Werner, H.-J.; Knowles, P. J.; Knizia, G.; Manby, F. R.; Schütz, M. and others; MOLPRO, version 2012.1, a package of ab initio programs, see <http://www.molpro.net>
- [19] Weigend, F.; Ahlrichs, R., *Phys. Chem. Chem. Phys.* **2005**, *7*, 3297-3305
- [20] Peterson, K. A.; Figgen, D.; Goll, E.; Stoll, H.; Dolg, M., *J. Chem. Phys.* **2003**, *119*, 11113-11123.
- [21] Azhary, A. E.; Rauhut, G.; Pulay, P.; Werner, H.-J., *J. Chem. Phys.* **1998**, *108*, 5185-5193.
- [22] Walsh, R. B.; Padgett, C. W.; Metrangolo, P.; Resnati, G.; Hanks, T. W.; Pennington, W. T. *Cryst. Growth Des.* **2001**, *1*, 165-175.
- [23] Zhu, W.; Zheng, R.; Zhen, Y.; Yu, Z.; Dong, H.; Fu, H.; Shi, Q.; Hu, W., *J. Am. Chem. Soc.* **2015**, *137*, 11038-11046.
- [24] Cinčić, D.; Friščić, T.; Jones, W. *Chem. Eur. J.* **2008**, *14*, 747-753.
- [25] Ji, B.; Wang, W.; Deng, D.; Zhang, Y., *Cryst. Growth Des.* **2011**, *11*, 3622-3628.
- [26] Stilinović, V.; Grgurić, T.; Piteša, T.; Nemeč, V.; Cinčić, D., *Cryst. Growth Des.* **2019**, *19*, 1245-1256.
- [27] Messina, M. T.; Metrangolo, P.; Resnati, G.; Quici, S.; Manfredi, A.; Pilati, T., *Supramol. Chem.* **2001**, *12*, 405-410.
- [28] Ji, B.; Wang, W.; Deng, D.; Zhang, Y.; Cao, L.; Zhou, L.; Ruan, C.; Li, T., *CrystEngComm.* **2013**, *15*, 769-774.
- [29] DeHaven, B. A.; Chen, A. L.; Shimizu, E. A.; Salpage, S. R.; Smith, M. D.; Shimizu, L. S. *Supramol. Chem.*, **2017**,
- [30] Gao, H. Y.; Shen, Q. J.; Zhao, X. R.; Yan, X. Q.; Pang, X.; Jin, W. J., *J. Mater. Chem.*, **2012**, *22*, 5336 – 5343.
- [31] Hakkert, S. B.; Grafenstein, J.; Erdelyi, M., *Faraday Discuss.* **2017**, *203*, 333-346

Graphic for Table of contents

